Journal of Muscle Research and Cell Motility **25**: 527–537, 2004.

Conformational changes in actin–myosin isoforms probed by Ni(II)·Gly–Gly–His reactivity

JULIETTE VAN DIJK[1], CHRYSTEL LAFONT[1], MENNO L.W. KNETSCH[2], JEAN DERANCOURT[1], DIETMAR J. MANSTEIN[2], ERIC C. LONG[3] and PATRICK CHAUSSEPIED[1,*]
[1]*CRBM du CNRS, 1919 Route de Mende, 34293 Montpellier, France;* [2]*Institute for Biophysical Chemistry, OE 4350, Hannover Medical School Carl-Neuberg-Straße 1, D-30623 Hannover, Germany;* [3]*Department of Chemistry, Indiana University-Purdue University Indianapolis, Indianapolis, IN 46202-3274, USA*

Received 29 June 2004; accepted in revised form 31 August 2004

Abstract

Crucial information concerning conformational changes that occur during the mechanochemical cycle of actin–myosin complexes is lacking due to the difficulties encountered in obtaining their three-dimensional structures. To obtain such information, we employed a solution-based approach through the reaction of Ni(II)·tripeptide chelates which are able to induce protein cleavage and cross-linking reactions. Three different myosin motor domain isoforms in the presence of actin and nucleotides were treated with a library of Ni(II)·tripeptide chelates and two reactivities were observed: (1) muscle motor domains were cross-linked to actin, as also observed for the skeletal muscle isoform, while (2) the *Dictyostelium discoideum* motor domain was cleaved at a single locus. All Ni(II)·tripeptide chelates tested generated identical reaction products, with Ni(II)·Gly–Gly–His, containing a C-terminal carboxylate, exhibiting the highest reactivity. Mass spectrometric analysis showed that protein cleavage occurred within segment 242–265 of the *Dictyostelium discoideum* myosin heavy chain sequence, while the skeletal myosin cross-linking site was as localized previously within segment 506–561. Using a fusion protein consisting of the yellow and cyan variants of green fluorescent protein linked by *Dictyostelium discoideum* myosin segment 242–265, we demonstrated that the primary sequence of this segment alone is not a sufficient substrate for Ni(II)·Gly–Gly–His-induced cleavage. Importantly, the cross-linking and cleavage reactions both exhibited specific structural sensitivities to the nature of the nucleotide bound to the active site, validating the conformational changes suggested from crystallographic data of the actin-free myosin motor domain.

Abbreviations: CFP, YFP, cyan and yellow variant of green fluorescent protein; ChamGGH, YFP–CFP chameleon fusion protein linked by the 242–265 segment residues of *Dictyostelium discoideum* myosin II; ChamTEV, YFP–CFP fusion protein linked by a 15 amino acid linker containing the cleavage site of rTEV protease; FRET, fluorescence resonance energy transfer; MMPP, magnesium monoperoxyphthalic acid; S1, myosin subfragment 1; M765, skS1 and smS1, motor domains from *Dictyostelium discoideum* myosin II (residues 1–765), skeletal muscle myosin and smooth muscle myosin, respectively.

Introduction

Conformational changes that occur within the actin–myosin complex during myosin ATPase activity are the origin of a great variety of cell movements. Through crystallographic structures of the myosin motor domains obtained in the presence of various nucleotide analogues, two extreme, closed and open, conformations of the nucleotide-binding pocket have been identified (Rayment *et al.*, 1993a; Fisher *et al.*, 1995; Smith and Rayment, 1996; Dominguez *et al.*, 1998; Houdusse *et al.*, 1999). In addition, with two recent structures proposed to mimic nucleotide-free myosin motor domain (Coureux *et al.*, 2003; Reubold *et al.*, 2003), it is now clearly established how changes induced by ATP binding and hydrolysis direct the position of the force-generating lever-arm that corresponds to the C-terminal long α-helical structure (see Houdusse and Sweeney, 2001 for a recent review). Unfortunately, even in light of the structures described above, the changes relevant to actin binding to myosin are much less supported by high resolution data. The recent three-dimensional structure of non-muscle myosin V obtained in the absence of nucleotide was proposed to mimic the actin binding state (Coureux *et al.*, 2003); this structure is characterized by the total opening of the nucleotide binding site and the closure of the so-called actin binding cleft together with the movement of the lever arm expected for an actomyosin binding complex. Due to the filamentous nature of actin, but also to the fact that the non-polymerized actin–myosin motor domain

*To whom correspondence should be addressed: Tel.: 33-467613334; Fax: +33-467521559; E-mail: patrick.chaussepied@crbm.cnrs.fr

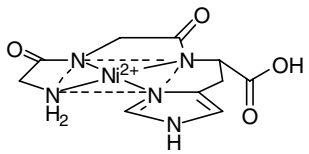

Ni(II)·Gly–Gly–His

complexes are inactive (Lheureux and Chaussepied, 1995), we do not expect a high resolution structure of an actin–myosin complex soon. To assist, therefore, in confirming the data obtained with the nucleotide-free myosin motor domain, and its relevance to actin binding, we have taken a solution-based approach to examine actin–myosin complexes through the use of Ni(II)·Gly–Gly–His metallopeptides.

Peptides of the general form Xaa–Xaa–His bind avidly to Cu(II) or Ni(II) forming 1:1 complexes via their terminal amines, two intervening deprotonated amides and the His imidazole (Harford and Sarkar, 1997). The tripeptide nickel chelates so-formed exhibit reactivities that can be applied as tools in the biochemical analysis of protein–nucleic acid and protein–protein interactions. For example, Gly–Gly–His fused to DNA binding proteins (or motifs) promote rapid and efficient DNA cleavage specifically at their DNA binding sites in the presence of Ni(II) and a strong oxidant (Mack and Dervan, 1990; 1992; Nagaoka *et al*., 1994; Harford *et al*., 1996; Long *et al*., 2003). Along with nucleic acid modification, intra- and inter-molecular protein cross-linking reactions are observed *in vitro* by adding Ni(II)·Gly–Gly–His under oxidative conditions to a protein (or a protein mixture) or by fusing the tripeptide to a recombinant protein (Brown *et al*., 1995; 1998; Bertrand *et al*., 1997). In addition to these two reactions, Cuenoud *et al*., reported that Ni(II)·Gly–Gly–His cleaves calmodulin at a single locus when the reagent is attached either to trifluoroperazine, a calmodulin binding inhibitor, or to the single cysteine of calmodulin (Cuenoud *et al*., 1992).

In general, Ni(II)·Gly–Gly–His-derived metallo peptides are reactive either in the presence of molecular oxygen (Bal *et al*., 1994) or upon activation with exogenous oxidants leading to a non-diffusible radical species that, in the case of DNA substrates (Liang *et al*., 1998), can abstract a C4′-hydrogen atom from the deoxyribose backbone. During protein cross-linking reactions, Ni(II)·Gly–Gly–His is proposed to target primary aromatic amino acids (Brown *et al*., 1995), making it a very attractive reagent since most available zero-length protein cross-linkers involve nucleophilic amino acids. As an example, Ni(II)·Gly–Gly–His was used to investigate the hydrophobic interface between actin and skeletal muscle myosin subfragment 1 (skS1) (Bertrand *et al*., 1997); upon their reaction, a covalent actin–skS1 complex was formed. Interestingly, the actin and/or skS1 residues cross-linked in this complex vary depending on the nature of the nucleotide bound to the active site of S1. Ni(II)·Gly–Gly–His was thus able to reveal conformational changes not described previously in the hydrophobic actomyosin interface during ATP hydrolysis (Geeves and Conibear, 1995; Van Dijk *et al*., 1998).

In the present work, the reaction of tripeptide nickel chelates was applied to two additional myosin isoforms, smooth muscle myosin and *Dictyostelium discoideum* myosin II. Further, the reactivity of the metallotri peptide was examined by using two tripeptide libraries of the general form Xaa–Xaa–His employed previously to improve DNA cleavage (Huang *et al*., 1999). The results showed that Ni(II)·Gly–Gly–His, which remained the most reactive metallotripeptide, induces *cross-linking* between actin and muscle myosin motor domains and a *cleavage* of the *Dictyostelium discoideum* motor domain regardless of the presence of actin. Cleavage occurred at a very specific site within the *Dictyostelium discoideum* myosin heavy chain which differs from the site involved in muscle S1 cross-linking with actin, but both cross-linking and cleavage reactions were found to be sensitive to the nature of the nucleotide bound to the active site. These results provide information on conformational changes that occur in the various S1 isoforms during the mechanochemical cycle of the actomyosin complexes and, in a more general way, show the benefit of using Ni(II)·metallopeptide reactions to investigate conformational changes in proteins during active turnover.

Materials and methods

Purification of muscle proteins

Rabbit skeletal F-actin was prepared from acetone powder and further purified by two cycles of polymerization–depolymerization (Eisenberg and Kielley, 1974). Skeletal muscle myosin subfragment 1 (skS1) was prepared from rabbit muscle after chymotryptic digestion of myosin filaments (Offer *et al*., 1973; Weeds and Taylor, 1975). Smooth muscle myosin subfragment 1 (smS1) was prepared after papain proteolysis of chicken gizzard muscle myosin, as reported (Marianne-Pepin *et al*., 1983). Protein concentrations were determined spectrophotometrically using extinction coefficients of $A^{1\%}{}_{280\ nm}$=11.0 cm^{-1} for actin, 5.7 cm^{-1} for skeletal muscle myosin, 7.5 cm^{-1} for skS1, and 4.5 cm^{-1} for smooth muscle myosin. The concentration of smS1 was estimated by the method of Bradford (Bradford, 1976). The molecular masses used were 42, 500, 115 and 135 kDa for actin, skeletal muscle myosin, skS1 and smS1 respectively.

Production and purification of recombinant proteins

The *Dictyostelium discoideum* motor domain (M765, corresponding to residues 1–765) fused to a polyhistidine tag was expressed in *Dictyostelium discoideum* and purified as described by Manstein and Hunt (Manstein

and Hunt, 1995). A plasmid encoding FLAG-tagged M765 was generated by subcloning M765 into vector PDXA-3FLAG, as described (Knetsch *et al.*, 2003). FLAG-tagged M765 was transformed and expressed into *Dictyostelium* and purified using an anti-FLAG-M2-agarose column and 3XFLAG peptide was used for elution. The concentration of M765 was estimated by the method of Bradford (Bradford, 1976) using a molecular mass of 88 kDa.

Multistep cloning strategies were used to create fusion proteins of YFP and CFP linked by segment 242–265 of M765 (ChamGGH) or by the rTEV target site (ChamTEV). The coding sequence of YFP was amplified from pEYFP-N1 (Clontech) by PCR and cloned between the Nhe 1 and Hind III restriction sites of pECFP-N1 (Clontech). A DNA fragment encoding the linker region (amino acid sequence, FIEIQFNNAGFISGASIQSY LLEK for ChamGGH and IEGRENLYFQGD for ChamTEV) was inserted between the Hind III and Bam H1 restriction sites located between YFP and CFP. The constructs generated were cloned into the Nhe 1 and Not 1 restriction sites of the bacterial expression vector pET28c (Invitrogen) downstream of the polyhistidine tag. Final constructs were transformed and expressed into *Escherichia coli* BL21(DE3). Purification was performed by Ni-affinity on Ni-NTA superflow from Qiagen according to the manufacturer's procedure. After purification, the proteins were extensively dialysed against the Ni(II)·Gly–Gly–His reaction buffer (BufferGGH: 50 mM Tris, 50 mM NaCl, 2 mM $MgCl_2$, pH 7.5). Protein concentrations were determined by using $\varepsilon_{513\ nm}$= 36,500 M^{-1} cm^{-1} for YFP along with Bradford's assay. The molecular masses used were 59 and 60 kDa for ChamTEV and ChamGGH, respectively.

Ni(II)·tripeptide induced modification of S1 or F-actin–S1 complexes

S1 (50 μM) in BufferGGH was incubated in the presence of 1 mM Ni(II)·tripeptide alone (from a freshly prepared concentrated aqueous solution containing stoichiometric concentrations of nickel and tripeptide) or in the presence of 50 μM actin and/or 2 mM ADP, ATP, ADP·BeF_x, ADP·AlF_4, PPi, or AMPPNP added prior to the addition of Ni(II)·tripeptide. After a 1 min incubation, 1 mM MMPP was added and the chemical reaction was stopped after 1 min by addition of a two-fold excess of boiling Laemmli's solution (Laemmli, 1970). Samples were then subjected to SDS–PAGE analysis. The tripeptide used was either Gly–Gly–His (with a free carboxy- or an amidated carboxy-terminus) or one member of a combinatorial tripeptide library of C-terminal amidated tripeptides [Xaa–Xaa–His, where one Xaa amino acid is a specifically defined L-α-amino acid (excluding Cys and Trp) and the other Xaa is any one of 18 naturally occurring L-α-amino acids (excluding Cys and Trp)], synthesized as described previously (Huang *et al.*, 1999).

Cleavage of ChamGGH and ChamTEV by Ni(II)·Gly–Gly–His or rTEV protease

Cleavage of 8 μM ChamGGH or ChamTEV was performed at 25 °C in BufferGGH with 1 mM Ni(II)·Gly–Gly–His and 1 mM MMPP or with 100 units of rTEV protease. Before the addition of the cleavage reagent, and after a 1 min reaction with Ni(II)·Gly–Gly–His or a 2 h reaction with rTEV, fluorescence emission spectra were recorded and 20 μl samples were withdrawn and mixed with 20 μl of Laemmli Buffer (Laemmli, 1970).

Fluorescence measurements

Fluorescence measurements were carried out on a C-16 Quantamaster PTI fluorimeter. Emission spectra were monitored at 25 °C from 450 nm to 600 nm with an excitation wavelength of 425 nm.

SDS-PAGE and western blotting

Gel electrophoresis was performed as described by Laemmli using a 4–18% gradient acrylamide gel and stained with Coomassie Blue. Densitometric analysis of the gels was carried out with a Shimadzu CS 930 high-resolution gel scanner equipped with a computerised integrator.

Western blot studies were performed after electrophoretic transfer from acrylamide gels to nitrocellulose sheets as described previously (Towbin *et al.*, 1979). The polyclonal anti-actin antibodies were directed against the N-terminal 1–12 residues of actin and the antibody used to reveal skS1 and smS1 was directed against the N-terminal 27 kDa tryptic fragment of the skS1 heavy chain (Bonafé *et al.*, 1993). M765 was immunoblotted with a commercial anti-polyhistidine antibody. Protein bands were visualised by a secondary anti-IgG antibody conjugated to horseradish peroxidase using α-naphthol or luminol as substrate.

Mass spectrometric analysis

The fragments of M765 generated by Ni(II)·Gly–Gly–His were separated by excision from an SDS–PAGE gel and digested with trypsin. Mass determination of the tryptic peptides generated was performed with a MALDI-TOF mass spectrometer (Bruker). Masses were matched with the masses calculated from the M765 primary sequence taking into account trypsin miscleavage.

Results

Ni(II)·tripeptide promoted reactions with rigor actin–S1 complexes

In the presence of a strong oxidant, Ni(II)·Gly–Gly–His induces a covalent cross-link at the hydrophobic

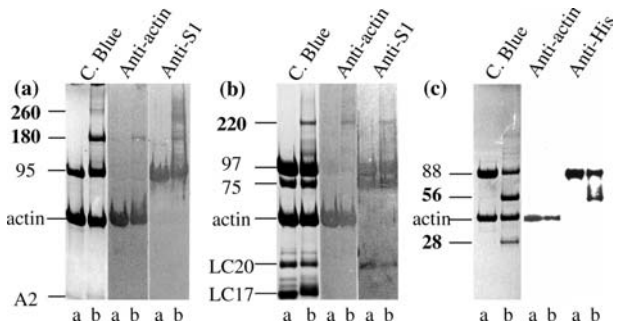

Fig. 1. Ni(II)·Gly–Gly–His reaction on rigor actin–S1 complexes. 50 μM actin was mixed with 50 μM skS1 (a), smS1 (b) or M765 (c) and 1 mM Ni(II)·Gly–Gly–His as described in Materials and methods. Samples were analysed on Coomassie Blue stained SDS–polyacrylamide gels before (a) and after (b) a 1-min incubation with 1 mM MMPP. For muscle S1 isoforms, the gel was immunoblotted with antibodies directed against actin or S1 heavy chain and revealed by a secondary anti-IgG antibody conjugated to horseradish peroxidase, using α-naphthol as a substrate. For M765, the gel was immunoblotted with antibodies against actin or the C-terminal polyhistidine tag of M765 and revealed by ECL (see Materials and methods).

interface between F-actin and skeletal muscle S1 (Bertrand *et al.*, 1997). In order to compare the interface formed between actin and different myosin isoforms, we performed the same Ni(II)·Gly–Gly–His treatment of actin complexed with skeletal muscle (skS1), smooth muscle (smS1) or *Dictyostelium discoideum* (M765) myosin motor domain.

Skeletal muscle S1 (skS1) is composed of part of myosin heavy chain (95 kDa fragment) and A2 light chain (Figure 1a, lane a). Ni(II)·Gly–Gly–His induced reaction on skS1 bound to actin generated two cross-linked products of 180 and 260 kDa, as described previously (Figure 1a, lane b) (Bertrand *et al.*, 1997). The covalent product of 260 kDa reacted only with anti 95 kDa antibodies and was identified as a covalent skS1 heavy chain oligomer. The product of 180 kDa corresponds to a cross-linked actin–skS1 complex, since it reacts with both anti-actin and anti-skS1 antibodies. Extensive peptide mapping showed that the cross-linking occurs between actin residues 48–113 and skS1 heavy chain residues 506–561 (Bertrand *et al.*, 1997).

Smooth muscle S1 (smS1), prepared by papain digestion of chicken gizzard myosin filaments, contains two light chains (LC17 and LC20) in addition to the 97 kDa fragment corresponding to residues 1–855 of the myosin heavy chain. A 75 kDa band also appears on SDS–PAGE resulting from uncontrolled cleavage of the 97 kDa fragment (Figure 1b, lane a). Upon Ni(II)·Gly–Gly–His treatment of the smS1–actin complex, a major 220 kDa product was formed (Figure 1b, lane b). Like the 180 kDa product obtained with skS1, western blotting revealed that the 220 kDa band contains both actin and smS1 and corresponds to a covalent actin–smS1 complex.

In contrast to the high molecular weight cross-linked products observed for muscle S1 isoforms, the reaction of Ni(II)·Gly–Gly–His with M765 (*Dictyostelium discoideum* myosin residues 1–765) bound to actin generated two low molecular weight bands of 28 and 56 kDa (Figure 1c). An antibody directed against actin labelled neither of these two bands. Since the entire M765 molecule has a molecular weight of 88 kDa, and since the amount of M765 dramatically decreased with the formation of the 28 and 56 kDa bands, we propose that the two reaction products arose from the cleavage of the M765 heavy chain. An antibody directed against the polyhistidine tag fused to the C-terminus of the M765 heavy chain illuminated only the 56 kDa band showing that the cleavage occurred 56 kDa from the C-terminus of M765 (Figure 1c). All three components of the reaction, Ni^{2+}, Gly–Gly–His and MMPP, were necessary for this cleavage reaction since the removal of any one of them prevented M765 degradation (data not shown). Furthermore, since Ni^{2+} is well known to display a high affinity for histidine residues, we investigated whether the cleavage was related to the presence of the polyhistidine tag on M765. Identical experiments performed with M765 molecule tagged with the flag peptide instead of the polyHis-tag generated the same cleavage, excluding the involvement of the histidine-containing tag during the reaction (data not shown).

Identification of the Ni(II)·Gly–Gly–His cleavage site in Dictyostelium discoideum myosin M765

To identify the cleavage site along M765, we attempted a sequence determination of the 28 and 56 kDa fragments but neither of them yielded a sequence when subjected to automated Edman degradation. This result, which was also reported after cleavage of calmodulin by Ni(II)·Gly–Gly–His (Cuenoud *et al.*, 1992), suggests the formation of a chemically modified N-terminus within the cleaved fragment during or after the reaction. A more precise localization of the cleavage site was achieved by comparison of mass spectrometry profiles of the tryptic digests of the two fragments. Mass spectrometric analysis of the tryptic digest of the 28 kDa fragment revealed peptides contained between amino acids 1 and 229, while within the 56 kDa tryptic digest, we detected peptides covering amino acids 268–765. The tryptic peptide corresponding to residues 242–265 with a mass of 2690 Da never appeared during the analysis. In light of the above data, we propose that the site of Ni(II)·Gly–Gly–His induced cleavage is localised within this highly hydrophobic segment 242–265 of the M765 heavy chain. This conclusion is consistent with the good correlation found between the apparent electrophoretic molecular weights of 28 and 56 kDa, and the resulting theoretical molecular weights of 27.6 and 57.8 kDa, respectively.

We further examined the properties of this cleavage site through an experiment in which a DNA strand encoding segment 242–265 was inserted between the DNA sequences coding for YFP and CFP fluorescent proteins, generating a so-called chameleon ChamGGH protein. In a situation where the primary sequence of segment 242–265 is sufficient for the Ni(II)·Gly–Gly–His

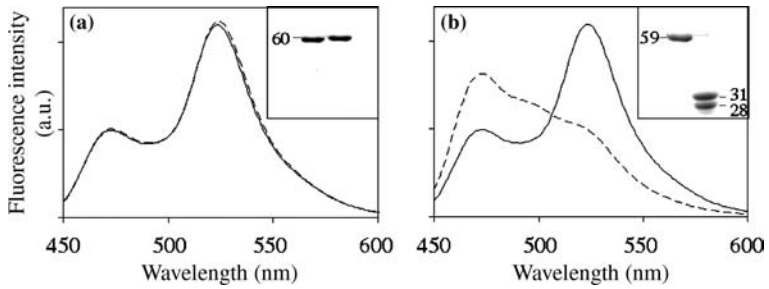

Fig. 2. Ni(II)·Gly–Gly–His reaction and rTEV proteolysis of ChamGGH and ChamTEV, respectively. (a) 8 μM ChamGGH was treated for one min with 1 mM Ni(II)·Gly–Gly–His and 1 mM MMPP. (b) 8 μM ChamTEV was treated with rTEV protease for 2 h. The insets show the Coomassie Blue stained gels of the protein content before (first lane) and after (second lane) the reaction. The emission spectra are monitored from 450 to 600 nm by exciting the solution at 425 nm before (full line) and after the reaction (dotted line).

induced cleavage to occur, one would expect that breaking the linker sequence between YFP and CFP would result in a loss of the fluorescence energy transfer (FRET) between fluorescence donor, CFP and fluorescence acceptor, YFP. Figure 2a shows that the fluorescence emission spectra of ChamGGH were identical before (full line) and after (dotted line) Ni(II)·Gly–Gly–His treatment, with a minor peak at 475 nm corresponding to CFP's emission and a major peak at 527 nm for YFP's emission. This result suggested the absence of cleavage of the chameleon protein. Consistent with this observation, the SDS polyacrylamide gel pattern was unchanged before and after reaction, with a single 60 kDa band corresponding to the expected ChamGGH molecular weight (Figure 2a, inset). As a control for the usefulness of this experimental approach, the same experiment was performed with a different chameleon YFP–CFP protein containing an rTEV protease sensitive linker (ChamTEV). As reported in Figure 2b, rTEV digestion of ChamTEV almost totally abolished YFP fluorescence emission at 527 nm whereas CFP emission at 475 nm was enhanced, presumably due to the fact that its excited state was no longer quenched by YFP. Accordingly, two bands of 31 and 28 kDa, corresponding to YFP and CFP, respectively, appeared on SDS gels after the cleavage reaction (Figure 2b, inset). Additional experiments showed that ChamGGH and ChamTEV still produced FRET after treatment with rTEV and Ni(II)·Gly–Gly–His respectively, indicating that those fusion proteins were also not cleaved (data not shown). These results confirm that the primary sequence of segment 242–265 alone is not sufficient for Ni(II)·Gly–Gly–His-induced cleavage and strongly suggest that this cleavage reaction is highly dependent on the protein conformation surrounding the 242–265 segment of native, intact M765.

Optimization of the Ni(II)·tripeptide reactions

In addition to the nature of the products of the Ni(II)·Gly–Gly–His reaction, the efficiency of the reaction is also significantly different between muscle and *Dictyostelium discoideum* myosin motor domains. Less than 15% of the muscle S1 molecules were cross-linked to actin while about 60% of M765 were cleaved in the presence of Ni(II)·Gly–Gly–His and MMPP under identical experimental conditions (Figure 1). This difference in yield could result from the fact that in the case of the cross-linking reaction (for muscle S1) the reagent is required to modify both S1 and actin. However, increasing the concentration of the reagents or the incubation time had no effect on the amount of cross-linked or cleaved S1. This observation suggests the existence of a competitive deactivation/degradation of the reagents which might be predominant in the case of muscle actin–S1 complexes.

In an attempt to optimise the actin–S1 cross-linking and cleavage reactions and to potentially gain information on their molecular mechanisms, we treated each protein complex with two NH_2–Xaa–Xaa–His–$CONH_2$ tripeptide libraries in which the first (Xaa_1) or the second (Xaa_2) amino acid was defined systematically while the remaining, undefined position contained an equal representation of the remaining 18 L-α-amino acids employed (Huang *et al.*, 1999). With all tripeptides tested, the products of each reaction were identical to those obtained with Gly–Gly–His, i.e., a cross-linked complex in the presence of muscle S1 and a cleavage reaction with *Dictyostelium discoideum* myosin motor domain (data not shown). However, by quantifying the amount of cross-linked or cleaved products, we observed significant differences in the reactivity of the tripeptides as a function of their amino acid compositions (Figure 3).

Of immediate note, presence of a C-terminal peptide amide decreased the amount of muscle S1 cross-linking by 15–17%, while having only a minor effect (less than 4%) on the cleavage of M765 (Figure 3, acid vs. amide bars). In addition, it was found that the yields of cross-linked products obtained with skS1 and smS1 were strongly dependent on the nature of the amino acid residues located in both the first and second peptide positions of Ni(II)·Xaa–Xaa–His. However, none of the tripeptides tested exhibited a higher reactivity than Gly–Gly–His–COOH. Interestingly, simple visual inspection of the histograms in Figure 3 indicated that the Xaa specificity of the cross-linking reaction differed between the two muscle myosin isoforms. Finally, the cleavage

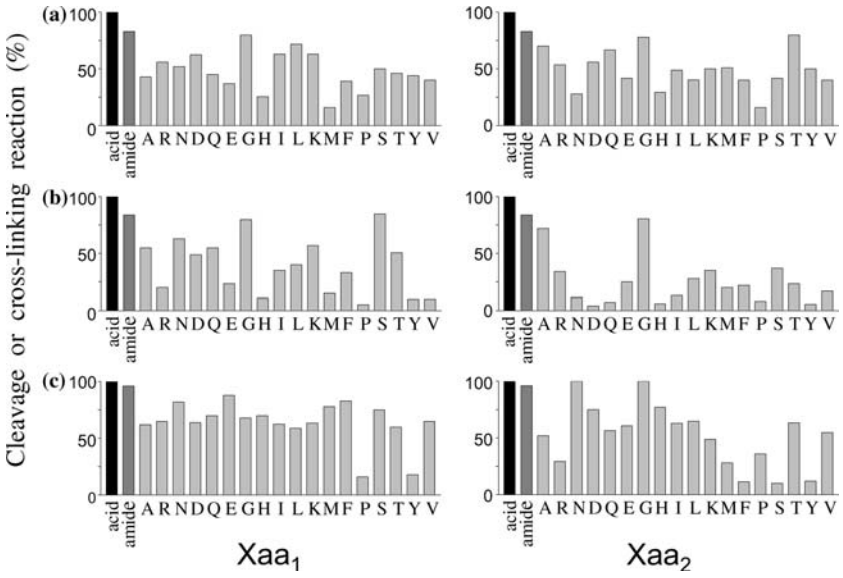

Fig. 3. Efficiency of Ni(II)·Xaa_1–Xaa_2–His tripeptides on the actin–S1 complexes. The reaction was conducted as described in the legend to Figure 1 using either Gly–Gly–His (acid form, first column or amide form, second column) or one of the C-terminal amide tripeptides issued from the libraries. The cross-linking efficiency for skS1 (a), and smS1 (b) and the cleavage efficiency for M765 (c) were monitored by estimating the amount of cross-linking and cleavage products on Coomassie Blue stained SDS–polyacrylamide gels. Results are reported in percentages relative to that obtained with the acid form of Gly–Gly–His. The left panels correspond to the library in which the Xaa_1 amino acid is specifically defined (using the single letter code) while Xaa_2 contains an equal representation of 18 naturally occurring L-α-amino acids (excluding Cys and Trp) (Huang *et al.*, 1999). In the right panels, the second amino acid, Xaa_2, is specifically defined while Xaa_1 contains an equal representation of 18 naturally occurring L-α-amino acids (excluding Cys and Trp).

reaction of M765 was observed to be less sensitive to the amino acid in the first Xaa position, except for the strong inhibitory effect of Pro and Tyr; this reaction is much more sensitive to the amino acid in the Xaa_2 position in which Gly and Asn were favoured.

Given the nature of these results, it is difficult to outline a set of general rules concerning the dependence of Ni(II)·Xaa–Xaa–His amino acid composition on the mechanism of the cross-linking or cleavage reactions since the most effective amino acids within the Xaa–Xaa–His peptide ligands tested did not share any common characteristic other than the presence of the C-terminal His residue and the overriding efficiency of Gly in the remaining tripeptide positions. In any case, these experiments revealed that the most efficient reagent on the actin–S1 complexes was Gly–Gly–His containing a C-terminal carboxylate. Therefore all further experiments were performed with the acid form of Gly–Gly–His.

Effect of nucleotides on the Ni(II)·Gly–Gly–His reaction with actin–S1 complexes

Since the structure of S1 or of the actin–S1 interface is sensitive to the nucleotide bound to the active site of S1, we investigated the effect of various nucleotide analogues on the Ni(II)·Gly–Gly–His-induced reaction. As demonstrated earlier by Bertrand and colleagues, the apparent molecular weight of 180 kDa of the skS1-containing cross-linked product obtained in the absence of nucleotide or in the presence of ADP, was shifted to 200 kDa in the presence of ATP or ADP·Pi analogues (AMPPNP, PPi, ADP·BeF_x and ADP·AlF_4; Figure 4a). The cross-linking sites involved in both covalent actin–skS1 adducts were mapped to S1 segment 506–561 and actin segment 48–113 using actin derivatives and proteolysed skS1 (Bertrand *et al.*, 1997). The difference in the apparent molecular weights between the complexes was proposed to result from different cross-linking sites within these segments.

Cross-linking of actin to smS1 was also found to be nucleotide sensitive (Figure 4b). While the covalent actin–smS1 complex of 220 kDa was formed in the

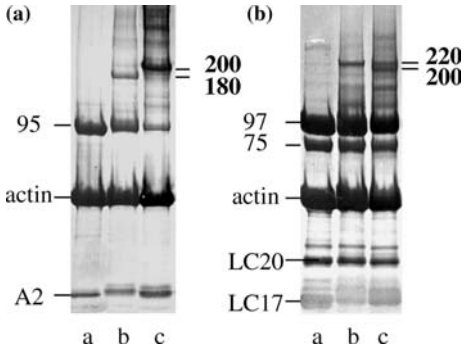

Fig. 4. Effect of nucleotide analogues on the Ni(II)·Gly–Gly–His–induced cross-linking of muscle actin–S1 complexes. 50 μM actin was incubated with skS1 (a) or smS1 (b) and treated for one min with 1 mM Ni(II)·Gly–Gly–His and 1 mM MMPP with no nucleotide or 2 mM ADP (lane b), or with 2 mM ATP, ADP.BeF_x, ADP.AlF_4, PPi, or AMPPNP (lane c with ATP). Lane a corresponds to the protein mixture before the addition of Ni(II)·Gly–Gly–His and MMPP. Samples were analysed by gel electrophoresis and stained with Coomassie Blue.

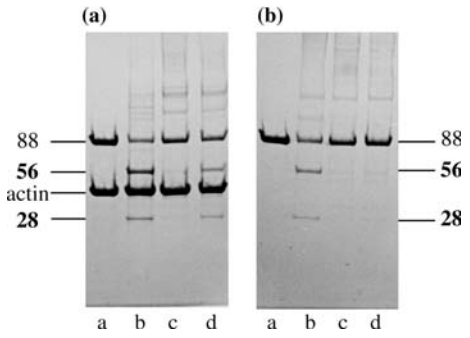

Fig. 5. Effect of nucleotide analogues on the Ni(II) · Gly–Gly–His–induced cleavage of M765. 50 μM M765 in the presence (a) or in the absence (b) of 50 μM actin was treated with 1 mM Ni(II)· Gly–Gly–His and 1 mM MMPP with either no nucleotide or 2 mM ADP (lane b), 2 mM ATP (lane c), or 2 mM ADP·BeF_x, ADP·AlF_4, PPi, or AMPPNP (lane d shows result with AMPPNP). The sample in lane a was withdrawn just before the addition of Ni(II) · Gly–Gly–His and MMPP. Samples were analysed by gel electrophoresis and stained with Coomassie Blue.

presence of all nucleotides, an additional cross-linked product of 200 kDa was generated only in the presence of ATP or ADP·Pi analogues. Although the nucleotide-induced shift in the molecular weight is different (opposite) between the skeletal and smooth S1 isoforms, these results confirm the sensitivity of the hydrophobic actin-myosin interface towards the presence of γ-phosphate-containing ligands in the muscle myosin active site.

The Ni(II)·Gly-Gly-His induced cleavage of M765 is also sensitive to the state of the nucleotide bound to the active site (Figure 5). However, only the yield of cleavage and not the nature of the generated fragments varied upon nucleotide binding to M765. When the reaction was performed on the actin–S1 complex (Figure 5a), cleavage was totally inhibited in the presence of ATP and decreased by 58% in the presence of ADPBeF_x, ADP·AlF_4, AMPPNP and PPi (with a 25% cleavage yield as compared to the 60% yield obtained in the absence of nucleotides). When M765 was treated in the absence of actin, a slightly lower yield of cleavage was observed in the presence of ADP and in the absence of nucleotide (50% vs. 60% in the presence of actin). ATP and its analogues totally inhibited the cleavage reaction of M765 in the absence of actin (Figure 5b; lanes c and d). This last result indicates that the nucleotide-induced inhibition observed in the presence of actin was clearly due to structural changes occurring in M765 upon ATP binding. The 25% cleavage yield observed on the actin–M765 complex in the presence of ATP analogues could result from a partial dissociation of the nucleotide in the presence of actin (Figure 5a, lane d; Werber *et al*., 1992; Bobkov *et al*., 1997). Taken together, these data confirm that the cleavage reaction is strongly conformation-dependent as first suggested by the results obtained with the chameleon constructs discussed above (Figure 2).

Discussion

By comparing three different myosin isoforms alone or associated with actin, this work highlights the specificity of Ni(II)·Gly–Gly–His reactions with proteins and their effectiveness in probing specific conformational changes in proteins and protein complexes.

Specificity of the Ni(II)·Gly–Gly–His reaction

Our results show that in the presence of MMPP, Ni(II)·Xaa–Xaa–His chelates react with actomyosin complexes in a myosin isoform-specific and nucleotide-state dependent way. Muscle S1 isoforms are cross-linked to actin while the *Dictyostelium* motor domain is cleaved at a single locus in its heavy chain. The S1 residues cross-linked to actin have been identified previously within segment 506–561 of skS1 (Bertrand *et al*., 1997). This segment is located in the lower 50 kDa domain and includes a helix–loop–helix motif (Pro529–His558) proposed to represent a hydrophobic part of the primary, stereo-specific actin binding site of skS1 (Figures 6 and 7) (Rayment *et al*., 1993b; Milligan 1996). We localised the cleavage site within segment

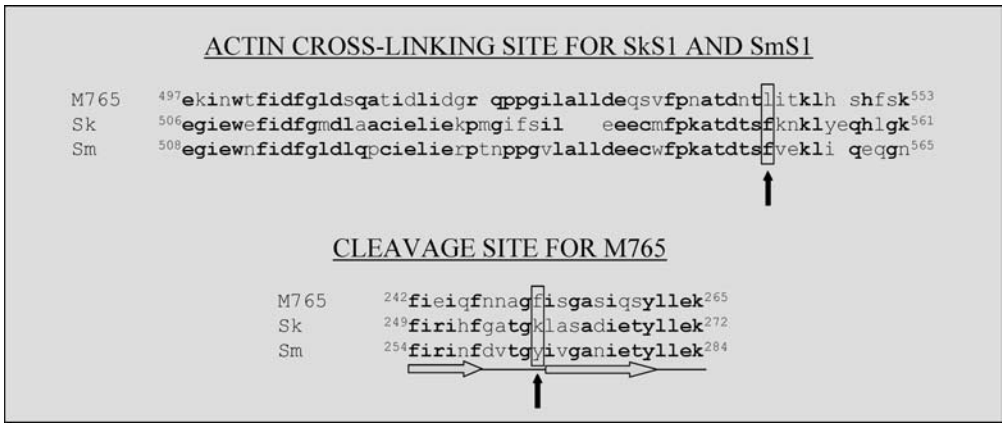

Fig. 6. Comparison of the primary sequences of the Ni(II)·Gly–Gly–His specific cross-linking and cleavage sites between the different S1 isoforms. Amino acids present in at least two of the three sequences are in bold. Arrows indicate potentially reactive Phe (F) residues. β-strands (horizontal arrows) and loops (lines) are noted below the cleaved segment.

242–265 of the M765 heavy chain. The primary sequence of this segment shares a 50 and 58% identity with the corresponding residues in skS1 (249–272) and in smS1 (254–284), respectively (Figure 6). Despite this relatively high primary sequence conservation, only M765 is cleaved in the Ni(II)·Gly–Gly–His-induced reaction.

Ni(II)·Gly–Gly–His has been proposed to induce radical formation in aromatic residues (Brown *et al.*, 1995). In good agreement with this idea, we identified aromatic residues likely involved in the cross-linking and cleavage reactions (Figure 6). A phenylalanine residue present in the cross-linked segment of SkS1 (Phe550) and SmS1 (Phe555) but not in the corresponding segment in M765 may participate in the muscle myosin isoform-specific cross-linking reaction. Phe252, present in the cleaved segment of M765 but absent in muscle S1 isoforms, is a plausible candidate for the cleavage reaction. A chimeric protein composed of two fluorescent proteins separated by segment 242–265 was not cleaved by Ni(II)·Gly–Gly–His, thus revealing that the presence of Phe252 alone, nor the nature of the primary sequence of segment 242–265, were sufficient to explain the specificity of the cleavage reaction. We therefore propose that amino acids surrounding the cleaved segment in the three-dimensional protein structure determine the specificity of the Ni(II)·Xaa–Xaa–His reaction. This proposal is in accordance with the results obtained with bovine brain calmodulin in which Ni(II)·Gly–Gly–His-induced cleavage occurred within segment 43–75 (second EF-hand) (Cuenoud *et al.*, 1992), which shares no significant primary sequence identity with the M765 cleavage segment described in this work.

Optimization of the Ni(II)·Gly–Gly–His reaction

In an attempt to optimise the Ni(II)·Gly–Gly–His induced reactions observed in this study, and to perhaps probe their mechanisms of action, we tested combinatorial tripeptide libraries of Xaa–Xaa–His ligands in which the first or the second amino acid positions were varied systematically. For all tripeptides tested, only the yield and not the nature of the products of their reaction with the proteins examined were changed. For both the cross-linking and the cleavage reactions, the tripeptide Gly–Gly–His, containing a C-terminal carboxylate, was revealed to be the most reactive. Unfortunately, no general rules concerning the mechanism of the cross-linking reaction could be discerned since the most effective amino acids did not appear to share a common characteristic. Note that in the case of B-form DNA cleavage the metallotripeptide Ni(II)·Pro–Lys–His exhibits the highest activity; this optimized reaction likely benefits from complementary hydrophobic and ionic contacts that are established between the metallotripeptide and DNA that stabilise the reagent in an advantageous binding orientation (Long and Claussen, 2003; Huang *et al.*, 1999).

The fact that general rules could not be established for the reaction with these proteins suggests that the reaction of Ni(II)·Gly–Gly–His with each protein complex is unique and results in a 'signature' pattern of selected Xaa amino acids influenced by the individual three dimensional environments of each protein cleavage or cross-linking site. Given that the highest level of activity was achieved in each instance with Gly residues, this result may also indicate that the reactivity of Ni(II)·Xaa–Xaa–His with the proteins examined may be negatively influenced by amino acids larger than Gly due to steric clashes with the protein substrates. Importantly, these results also suggest that the His imidazole and the N-terminal amine, H-bond donor functionalities common to all the metallopeptides tested, may be the main determinants of their reactivity with proteins, as is the case with the DNA minor groove (Fang *et al.*, 2004).

Conformational changes of the myosin motor domain upon nucleotide binding

All the Ni(II)·Gly–Gly–His-induced reactions performed on the actin–myosin complexes exhibited specific sensitivities toward the nature of the nucleotide bound to S1. With skeletal muscle S1, two different covalent actin–skS1 complexes were generated depending on the type of nucleotide bound to S1; a 180 kDa product was obtained in the absence of nucleotide or with ADP. In this case, the actin–skS1 complex is in a strong binding conformational state defined from kinetic studies as the R-state (Geeves and Conibear, 1995). In contrast, with γ-phosphate-containing ligands (ATP or ADP·Pi analogues), which define a weak binding or A-state, a 200 kDa product was generated. In both cases, myosin segment 506–561 (containing the proposed cross-linked residue Phe550) was found to be involved in the cross-linking reaction (Bertrand *et al.*, 1997). Based on a recent reconstruction of the actin–myosin complex using the 3-D structure of S1 obtained in the absence of bound nucleotide, residue Phe550 (see above) would be located within the interface between actin and the lower 50 kDa domain (Coureux *et al.*, 2003). This work suggests that Phe550, and in a more general view, the Phe550-containing helix of the lower 50 kDa domain changes its contacts with actin during the A- to R-state isomerization of the actin–myosin interface.

The cross-linking of actin to smS1 also revealed changes of the actin–myosin interface during the weak to strong binding states since, in addition to the covalent actin–smS1 complex of 220 kDa obtained in the absence of nucleotides or with ADP, a 200 kDa product was generated in the presence of ATP or ATP analogues. However, while the actin–skS1 interface was sensitive to the nucleotide in an all or none manner, the response of smS1 was mixed since with ATP or ADP·Pi analogues, the two types of cross-linked products were generated in approximately equal amounts. Though it is difficult to

rule out definitively the fact that ATP is partly consumed under our experimental conditions, these results could suggest that two types of actin–myosin interfaces coexist in the presence of ATP analogues. Together with other unusual actin binding properties of smooth muscle myosin (Whittaker *et al*., 1995), these results are likely to be involved in the force maintenance characterising this type of muscle.

For M765, both the nature of the nucleotide and the presence of actin affect the yield of heavy chain cleavage. Cleaved segment 242–265 follows switch I and has a strand-loop–strand-stretch structure (Figures 6 and 7). The two strands correspond to strand 6 and 7 of the seven-stranded β-sheet that couples the N-terminal region to the upper 50 kDa domain (Figure 7). Recent three-dimensional structures of the myosin motor domain obtained without bound nucleotide clearly show that strands 5–7 of this β-sheet undergo a distortion in the apo-state allowing a large movement of the upper 50 kDa domain, which results in closure of the 50 kDa cleft (Coureux *et al*., 2003; Reubold *et al*., 2003). However, the movement of the strands does not affect their H-bond pattern. Therefore, we do not expect cleavage to occur within these strands but rather within loop 248–252 or within stretch 262–265 which are flexible segments that may encompass changes in their electronic links. Since stretch 262–265 is completely conserved among the different myosin isoforms (Figure 6), it is unlikely to be specifically cleaved in *Dictyostelium discoideum* myosin. This analysis suggests that loop 248–252 contains the cleavage site, in good accordance with the presence of the non-muscle isoform specific Phe252 residue, as discussed above (Figure 6). It is important to note that loop 248–252 is surrounded in the 3-D structure by three other flexible loops: loop 166–172, loop 201–209 (also called loop 1) and loop 443–448 (Figure 7b). Interestingly, it is well established that loop 1 senses ATP hydrolysis and actin binding to S1 through changes in its proteolytic susceptibility (Applegate and Reisler, 1984; Mornet *et al*., 1985; Lheureux and Chaussepied, 1995) and the fact that it is more or less stabilized in the X-ray diffraction patterns depending on the nucleotide bound to S1 (Coureux *et al*., 2003). The size and the nature of loop 1 were correlated to the performance of the various myosin isoforms (Goodson *et al*., 1999). Note also that the effects observed on the proteolysis of loop 1 were different with actin, ADP and ATP in correlation with the sensitivity of the Ni(II)·Gly–Gly–His-induced cleavage which is enhanced by actin, unaffected by ADP, and inhibited by ATP and ADP·Pi. On the other hand, the loops formed by residues 166–172 and 443–448 also undergo distortions upon nucleotide binding (Whittaker *et al*., 1995; Coureux *et al*., 2003). The nucleotide- and actin-induced structural rearrangements of these three loops around loop 248–252 could change the reactivity of Phe 252 and/or the accessibility of Ni(II)·Gly–Gly–His to the cleaved residue. Altogether, these results suggest that the flexibility not only of loop 1 but of the set of these four loops is under the control of actin- or the type of nucleotide- bound to S1. This set of loops could represent a true hinge in the pathways of the catalytic and the actin binding sites which is fully active during the nucleotide-induced movement of the upper 50 kDa region.

In conclusion, our work has shown that the reactivity of proteins with Ni(II)·Xaa–Xaa–His can reveal conformational changes which are protein-specific and which can be different within the same protein family. This high specificity makes Ni(II)·Xaa–Xaa–His reactivity a very useful tool for discerning details of protein structure and function in the postgenomic area. To this end, expressing *in cellulo* a given protein fused to an Xaa–Xaa–His tripeptide-ligand could be a suitable method for the identification of intracellular partners by specifically cross-linking them to the fusion protein and for monitoring conformational changes during the activity of the fusion protein.

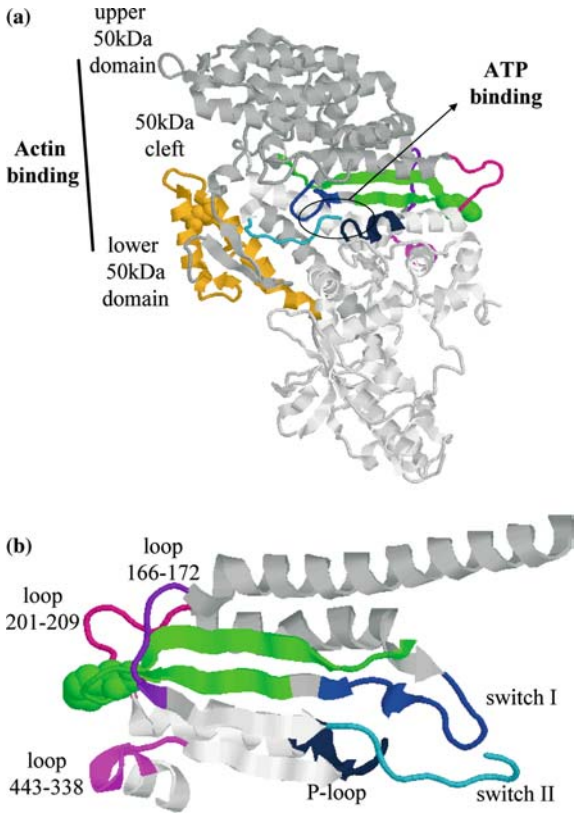

Fig. 7. Localization of the cross-linking and cleavage sites in the three-dimensional structure of the myosin motor domain. The structure of M765 in its apo state (Reubold *et al*., 2003) is shown either in a full view (a) or in an enlarged back view focused on the cleavage site (b). The 50 kDa fragments (dark grey) and the remainder of the molecule (light grey) are highlighted. The colour code is: cleavage site (segment 242–265), green; cross-linking site (segment 506–561), yellow; switch I (segment 229–240), blue; switch II (segment 455–464), light blue; P-loop (segment 179–187), dark blue; loop 1 (segment 201–209), magenta; loop 443–338, purple; loop 166–172, violet. $ATP_{\gamma}Pi$ and actin binding sites are shown. The two possible candidates for the cross-linking (Phe550, yellow) and the cleavage (Phe252, green) reactions are also indicated as space-filled segments.

Acknowledgements

We thank Georgios Tsiavaliaris (Hannover Medical School) for producing the Flag-tagged M765. This work was supported by CNRS and AFM to P.C., by NIH (GM62831) to E.C.L. and by DFG (Ma1081/5-3 and MA1081/6-1) to D.J.M.

References

Applegate D and Reisler E (1984) Nucleotide-induced changes in the proteolytically sensitive regions of myosin subfragment 1. *Biochemistry* **23:** 4779–4784.

Bal W, Djuran MI, Margerum DW, Gray ET, Mazid MA, Tom RT, Nieboer E and Sadler PJ (1994) Dioxygen-induced decarboxylation and hydroxylation of [Ni^{II}(glycyl–glycyl–L-histidine)] occurs via Ni^{III}: X-ray crystal structure of [Ni^{II}(glycyl–glycyl–hydroxy-D, L-histamine)]·$3H_2O$. *J Chem Soc, Chem Commun* 1889–1890.

Bertrand R, Derancourt J and Kassab R (1997) Probing the hydrophobic interactions in the skeletal actomyosin subfragment 1 and its nucleotide complexes by zero-length cross-linking with a nickel–peptide chelate. *Biochemistry* **36:** 9703–9714.

Bobkov AA, Sutoh K and Reisler E (1997) Nucleotide and actin binding properties of the isolated motor domain from *Dictyostelium discoideum* myosin. *J Muscle Res Cell Motility* **18:** 563–571.

Bonafe N, Chaussepied P, Capony JP, Derancourt J and Kassab R (1993) Photochemical cross-linking of the skeletal myosin head heavy chain to actin subdomain-1 at Arg95 and Arg28. *Eur J Biochem* **213:** 1243–1254.

Bradford MM (1976) A rapid and sensitive method for the quantitation of microgram quantities of protein utilising the principle of protein–dye binding. *Anal Biochem* **72:** 248–254.

Brown KC, Yang SH and Kodadek T (1995) Highly specific oxidative cross-linking of proteins mediated by a nickel–peptide complex. *Biochemistry* **34:** 4733–4739.

Brown KC, Yu Z, Burlingame AL and Craik CS (1998) Determining protein–protein interactions by oxidative cross-linking of a glycine–glycine–histidine fusion protein. *Biochemistry* **37:** 4397–4406.

Coureux PD, Wells AL, Menetrey J, Yengo CM, Morris CA, Sweeney HL and Houdusse A (2003) A structural state of the myosin V motor without bound nucleotide. *Nature* **425:** 419–423.

Cuenoud B, Tarasow TM and Schepartz A (1992) A new strategy for directed protein cleavage. *Tetrahedron Lett*. **33:** 895–898.

Dominguez R, Freyzon Y, Trybus KM and Cohen C (1998) Crystal structure of a vertebrate smooth muscle myosin motor domain and its complex with the essential light chain: visualization of the pre-power stroke state. *Cell* **94:** 555–571.

Eisenberg E and Kielley WW (1974) Column chromatographic separation and activity of the three, active troponin components with and without tropomyosin present. *J Biol Chem* **249:** 4742–4748.

Fang Y-Y, Ray BD, Claussen CA, Lipkowitz KB and Long EC (2004) Ni(II)·Arg–Gly–His–DNA interactions: investigations into the basis for minor-groove binding and recognition. *J Am Chem Soc* **126:** 5403–5412.

Fisher AJ, Smith CA, Thoden JB, Smith R, Sutoh K, Holden HM and Rayment I (1995) X-ray structures of the myosin motor domain of *Dictyostelium discoideum* complexed with MgADP·BeFx and MgADP·AlF4. *Biochemistry* **34:** 8960–8972.

Geeves MA and Conibear PB (1995) The role of three-state docking of S1 with actin in force generation. *Biophys J* **68:** 194S–201S.

Goodson HV, Warrick HM and Spudich JA (1999) Specialized conservation of surface loops of myosin: evidence that loops are involved in determining functional characteristics. *J Mol Biol* **287:** 173–185.

Harford C and Sarkar B (1997) Amino terminal Cu(II)- and Ni(II)-binding (ATCUN) motif of proteins and peptides: metal binding, DNA cleavage, and other properties. *Acc Chem Res* **30:** 123–130.

Harford C, Narindrasorasak S and Sarkar B (1996) The designed protein M(II)·Gly–Lys–His–Fos(138–211) specifically cleaves the AP-1 binding site containing DNA. *Biochemistry* **35:** 4271–4278.

Houdusse A and Sweeney HL (2001) Myosin motors: missing structures and hidden springs. *Curr Opin Struct Biol* **11:** 182–194.

Houdusse A, Kalabokis VN, Himmel D, Szent-Gyorgyi AG and Cohen C (1999) Atomic structure of scallop myosin subfragment S1 complexed with MgADP: a novel conformation of the myosin head. *Cell* **97:** 459–470.

Huang X, Pieczko ME and Long EC (1999) Combinatorial optimization of the DNA cleaving Ni(II)·Xaa–Xaa–His metallotri peptide domain. *Biochemistry* **38:** 2160–2166.

Knetsch ML, Tsiavaliaris G, Zimmermann S, Ruhl U and Manstein DJ (2003) Expression vectors for studying cytoskeletal proteins in *Dictyostelium discoideum*. *J Muscle Res Cell Motility* **23:** 605–611.

Laemmli UK (1970) Cleavage of structural proteins during the assembly of the head of bacteriophage T4. *Nature* **227:** 680–685.

Lheureux K and Chaussepied P (1995) Comparative studies of the monomeric and filamentous actin–myosin head complexes. *Biochemistry* **34:** 11435–11444.

Liang Q, Ananias DC and Long EC (1998) Ni(II)·Xaa–Xaa–His induced DNA cleavage: deoxyribose modification by a common "activated" intermediate derived from $KHSO_5$, MMPP, or H_2O_2. *J Am Chem Soc* **120:** 248–257.

Long EC and Claussen CA (2003) In Demeunynk M, Bailly C and Wilson WD (Eds), *DNA and RNA Binders: From Small Molecules to Drugs*, (pp. 88–125) Wiley–VCH.

Mack DP and Dervan PB (1990) Nickel-mediated sequence-specific oxidative cleavage of DNA by a designed metalloprotein. *J Am Chem Soc* **112:** 4604–4606.

Mack DP and Dervan PB (1992) Sequence-specific oxidative cleavage of DNA by a designed metalloprotein, Ni(II)·GGH(Hin139–190). *Biochemistry* **31:** 9399–9405.

Manstein DJ and Hunt DM (1995) Overexpression of myosin motor domains in *Dictyostelium*: screening of transformants and purification of the affinity tagged protein. *J Muscle Res Cell Motility* **16:** 325–332.

Marianne-Pepin T, Mornet D, Audemard E and Kassab R (1983) Structural and actin-binding properties of the trypsin-produced HMM and S1 from gizzard smooth muscle myosin. *FEBS Lett* **159:** 211–216.

Milligan RA (1996) Protein–protein interactions in the rigor acto myosin complex. *Proc Natl Acad Sci USA* **93:** 21–26.

Mornet D, Pantel P, Audemard E, Derancourt J and Kassab R (1985) Molecular movements promoted by metal nucleotides in the heavy-chain regions of myosin heads from skeletal muscle. *J Mol Biol* **183:** 479–89.

Nagaoka M, Hagihara M, Kuwahara J and Sugiura Y (1994) A novel zinc finger-based DNA cutter: biosynthetic design and highly selective DNA cleavage. *J Am Chem Soc* **116:** 4085–4086.

Offer G, Moos C and Starr R (1973) A new protein of the thick filaments of vertebrate skeletal myofibrils. Extractions, purification and characterization. *J Mol Biol* **74:** 653–676.

Rayment I, Hoden HM, Whittaker M, Yahn CB, Lorenz M, Holmes KC and Milligan RA (1993a) Three-dimensional structure of myosin subfragment-1: a molecular motor. *Science* **261:** 50–58.

Rayment I, Holden HM, Whittaker M, Yahn CB, Lorenz M, Holmes KC and Milligan RA (1993b) Structure of the actin–myosin complex and its implications for muscle contraction. *Science* **261:** 58–65.

Reubold TF, Eschenburg J, Becker A, Kull FJ and Manstein DJ (2003) A structural model for actin-induced nucleotide release in myosin. *Nat Struct Biol* **10:** 826–830.

Smith CA and Rayment I (1996) X-ray structure of the magnesium(II).ADP.vanadate complex of the *Dictyostelium discoideum*

myosin motor domain to 1.9 Å resolution. *Biochemistry* **35:** 5404–5417.

Towbin H, Staehelin T and Gordon J (1979) Electrophoretic transfer of proteins from polyacrylamide gels to nitrocellulose sheets: procedure and some applications. *Proc Natl Acad Sci USA* **76:** 4350–4354.

Van Dijk J, Fernandez C and Chaussepied P (1998) Effect of ATP analogues on the actin-myosin interface. *Biochemistry* **37:** 8385–8394.

Weeds AG and Taylor RS (1975) Separation of subfragment-1 isoenzymes from rabbit skeletal muscle myosin. *Nature* **257:** 54–56.

Werber MM, Peyser YM and Muhlrad A (1992) Characterization of stable beryllium fluoride, aluminium fluoride, and vanadate containing myosin subfragment 1-nucleotide complexes. *Biochemistry* **31:** 7190–7197.

Whittaker M, Wilson-Kubale, EM, Smith JE, Faust L, Milligan RA and Sweeney HL (1995) A 35-Å movement of smooth muscle myosin on ADP release. *Nature* **378:** 748–751.